21st International Symposium on
Mathematical Theory of Networks and Systems
July 7-11, 2014. Groningen, The Netherlands

A new view of anti-windup design for uncertain linear systems in the frequency domain

Ari Berger[1] and Per-Olof Gutman[2]

***Abstract*— This paper presents a somewhat new perspective on the stability problem for uncertain LTI feedback systems with actuator input amplitude saturation. The solution is obtained using the QFT theory and a 3 Dof non-interfering control structure. Describing function analysis is used as a criterion for closed loop stability and limit cycle avoidance, but the Circle or Popov criteria could also be employed. The novelty is the parametrization of the three degrees of freedom. Two examples are given. The first is a benchmark problem and a comparison is made with other proposed solutions. The second is an example which was implemented and tested on an X-Y linear stage used for nano-positioning applications. Design and implementation considerations are given.**

***Index Terms*— Uncertain LTI systems, Anti-windup, Describing Function, Limit cycles, Saturation.**

I. Introduction

Actuator limitations are a well known practical problem. A saturated actuator can cause the closed loop system, see e.g. fig. 1, to become unstable or exhibit limit cycles. A well known case for instability is integral windup which was first noticed in PID controllers [2]. In [3] it is shown that the integrator case is only a special case of a more general problem, such that all systems with relatively slow dynamics will experience windup problems under actuator constraints. Windup up is then interpreted as an inconsistency between the controller output and the states of the controller.

During the past few decades many solutions have been offered to design controllers for linear plants in the presence of actuator saturation. One of the earliest works [2] dealt with PID controller windup and is commonly known as anti-reset windup. In [4] this strategy is extended further to use the conditioning technique for bumpless transfer. In [5] a unified framework is proposed for the anti-windup solution.

The problem of stabilization becomes even harder when uncertainty is present in the plant. Using QFT [6], Horowitz suggested the control structure in fig. 2. The solution is obtained using a mixed frequency domain/time domain method to handle the windup problem [7]. Horowitz did not take into account plant uncertainty when designing the anti-windup compensator, but in [8] the problem is solved for the uncertain case of a Type-1 system. The key transfer function in Horowitz's design is $1/(1+L_n)$, where $L_n = PG + H$ is the linear transmission around the saturation element in fig. 2. The function $1/(1+L_n)$ plays a crucial role in the commutation from saturated to unsaturated mode. This observation leads to a solution for the G and H transfer functions. In [8] the solution demands absolute stability of L_n.

In [9], time domain constraints are transformed into the frequency domain for a class of RH_2 transfer functions, i.e stable, real-rational, strictly proper transfer functions, such that conditions for avoiding saturation are formulated. The 2 DoF structure in fig. 1 is used, and the controller G for linear and non-linear operation is designed in a single step. QFT is used to take the plant uncertainty into account and construct the Horowitz-Sidi bounds for the linear compensator design. In [10] limit cycle avoidance is analyzed with the use of Describing Function and the Circle Criterion. In addition to the uncertainty in the plant P, the describing function gain $N(A)$ is also taken into account as part of the open loop uncertainty and a robust design is performed in a 2 DoF structure, fig. 1. Also in [10], it is shown how the Circle Criterion gives Horowitz-Sidi bounds in Nichols chart for the QFT design. We note that the 2 DoF structure in fig. 1 does not make it possible to avoid limit cycling in conditionally stable system.

The 3 DoF control structure, fig. 3, was used by many authors to solve the robust stability problem, especially in the framework of QFT. The structure in fig. 3 is called "non-interfering" since in the non-saturating mode, the controller transfer function equals G. It is easily shown that the structures in figs. 2 and 3 are equivalent, with $C = G/(1-E)$, and $H = E/(1-E)$.

Using a non-interfering control structure, in [1] global stability is assured through the use of stability multipliers [11], taking into account plant uncertainties. In [12] the authors use the theory of Horowitz [7] to establish a non-overshooting closed-loop response under input saturation constraint for uncertain plants. See [13], [14] for excellent surveys regarding different anti-windup techniques for the uncertain plant case.

In this paper a new look at the limit cycle avoidance problem is presented, by regarding the Describing Function of the saturation element as a gain uncertainty in the open loop transmission, as in [10], and using the 3 DoF control structure in fig. 2, parameterized in such a way that its non-interfering property is exploited.

Limitations of the Describing Function as a limit cycle condition is given in [15]. In general the Describing Function gives a necessary condition for limit cycles avoidance. In many practical cases the Describing Function analysis is

[1]Ari Berger is with the Faculty of Civil and Environmental Engineering, Technion - Israel Institute of Technology, 32000 Haifa, Israel ari@technion.ac.il

[2]Per-Olof Gutman is with the Faculty of Civil and Environmental Engineering, Technion - Israel Institute of Technology, 32000 Haifa, Israel peo@technion.ac.il

ISBN: 978-90-367-6321-9

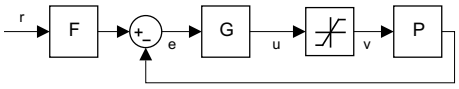

Fig. 1. A 2 DoF control structure with saturation

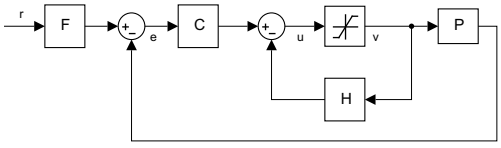

Fig. 2. The Horowitz 3 DoF control structure

useful [15], [16], [10] and gives a less conservative condition than global stability conditions, e.g the Popov and Circle Criteria.

The remainder of this paper is organized as follows. In section II the problem statement and required definitions are presented. In section III we define the Describing Function condition to avoid limit cycles, and the foundation for the solution is constructed. Section IV introduces our proposed solution. Section V shows a simulation-based design example and a comparison of the proposed solution with previous contributions from the literature. Section VI shows the results of an implementation of the proposed solution on a real system. In Section VII some design and implementation issues are addressed. Section VIII gives the conclusions.

II. Problem statement

Goal The problem to be solved is closed loop stability and limit-cycle avoidance in systems with actuator input amplitude saturation taking into account uncertainty in the plant. Our solution can be viewed as a new extension to [7], [10] and as a complement to [17], [18], [1], [8], [19].

Assumptions Two assumptions are made on the plant: it is an uncertain LTI system and it has no poles in the open right half plane. The control signal saturation limits are assumed to be known. Considering a unity saturation block, the input/output relation of the saturation element is defined as:

$$v(t) = \begin{cases} u(t) & \text{if } u(t) \in [-1, 1] \\ -1 & \text{if } u(t) < -1 \\ 1 & \text{if } u(t) > 1 \end{cases} \tag{1}$$

where $u(t)$ is the input to the saturation element and $v(t)$ is the output. In a real system there exist hardware and software saturation elements. The hardware is the true saturation of the actuator while the software reflects the one that the designer implements in the digital controller. It is assumed that the software saturation level is equal to or smaller than the hardware saturation level of the actuator. Since usually we do not have access to the saturation element in the actuator, this assumption will guarantee that the measured signal v, as defined in eq. (1), is not saturated further.

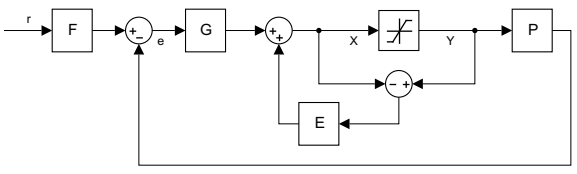

Fig. 3. A 3 DoF non-interfering control structure

Plant The plant to be controlled can be described as a member of a finite or infinite set of transfer functions

$$P(s) \in \{P_i(s)\} \tag{2}$$

One arbitrary transfer function from the set in eq. (2) is assigned as the nominal plant and is denoted by P_{nom}. In the following we will refer to the set $\{P_i(s)\}$ as $\{P\}$.

III. Method

First design step The design process starts as a classical linear QFT design problem using the 2 DoF control structure, fig. 1, for the unsaturated open loop transmission [20], [21], whereby G and F are designed. Considering the plant uncertainty, eq. (2), *templates* (frequency function value sets) are constructed. Horowitz-Sidi bounds are then computed based on some user defined specifications e.g tracking, disturbance rejection, closed loop bandwidth, etc. The nominal open loop transfer function is defined as

$$L_{nom} = P_{nom}G \tag{3}$$

where G is the feedback controller transfer function to be designed. Based on eq. (3), the control design in QFT proceeds as follows. Find $G(s)$ such that for each frequency ω [rad/sec]

$$L_{nom}(j\omega) \in B_r(\omega) \subset \mathbb{C} \tag{4}$$

where the feasible set $B_r(\omega)$ is generated with the help of specification no. r expressed in the frequency domain. The Horowitz-Sidi bounds $\partial B_r(\omega)$ are the boundaries of $B_r(\omega)$. If necessary and possible, the prefilter F is designed after G, such that the servo specifications are satisfied.

Frequency domain limit cycle avoidance criteria Use will be made of the describing function analysis for limit-cycle avoidance. The usage of the circle and Popov criterion for absolute stability assurance can also be used within the presented framework by formulating appropriate frequency domain constraints [18], [10]. From [15], the describing function of the saturation block, eq. (1), is given by

$$N(A) = \begin{cases} 1 & A \leq 1 \\ \frac{2}{\pi}\left[\arcsin\left(\frac{1}{A}\right) + \left(\frac{1}{A}\right)\sqrt{1-\left(\frac{1}{A}\right)^2}\right] & A > 1 \end{cases} \tag{5}$$

where A is the amplitude of the sine signal that enters the saturation. N(A) is the amplitude of the first harmonic of the output. There is no phase shift. The function is shown in fig. 4. Clearly, $\lim_{A\to\infty} N(A) = 0$, and

$$N(A) \in [0, 1] \tag{6}$$

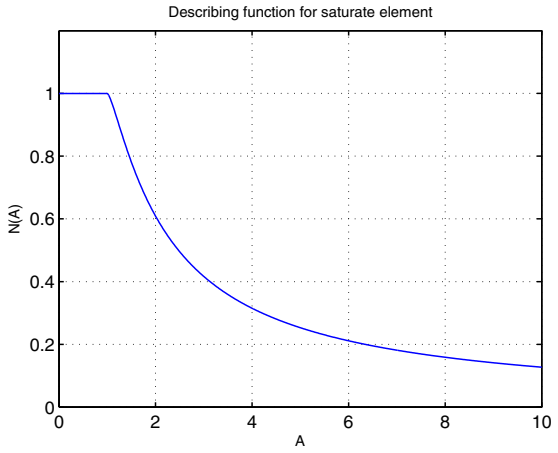

Fig. 4. Describing function of the saturation element $N(A)$ as a function of the sinusoidal input amplitude A.

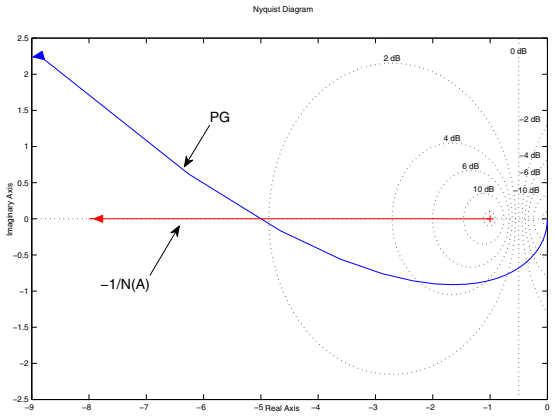

Fig. 5. Nyquist plot of the open loop $L = PG$ and the line $-1/N(A)$. The arrow on the PG-curve indicates increasing frequency, and the arrow on the -1/N-plot indicates increasing amplitudes.

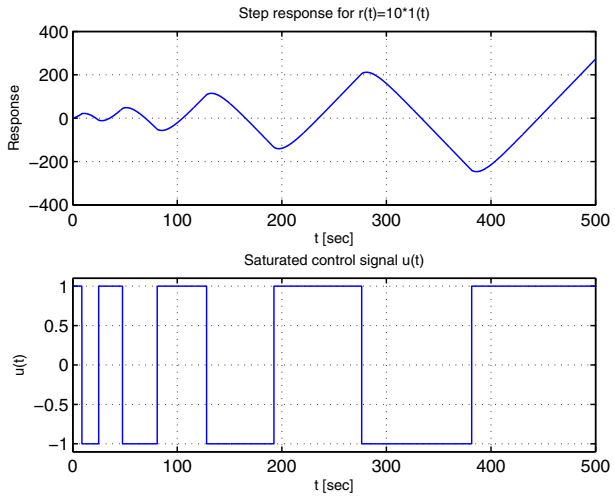

Fig. 6. Simulated closed loop response for a step reference $r(t) = 10*1(t)$.

which means that the saturation can be taken as an uncertain gain in the open loop transmission. The gain uncertainty defined by eq. (6) will be denoted as $\{N\}$.

In [15], section 3.1, Describing Function criteria for limit cycle avoidance are given. If the open loop frequency function around the non-linearity intersects $-1/N(A)$, limit cycles may appear if saturation occurs. Conditions for the stability of the limit cycles are also given. As an example, consider the plant P without uncertainty, feedback compensator G and pre-filter F

$$P = 5\frac{(s/0.7+1)}{s(s/0.04+1)}, \quad G = \frac{6s+5}{s}, \quad F = 1$$

configured according to fig. 1. The closed loop unsaturated system is conditionally stable. In fig. 5 the open loop $L = PG$ Nyquist plot is shown together with the locus of $-1/N(A)$. Since L intersects $-1/N(A)$ at some frequency, the closed loop system may exhibit a limit cycle, if the plant input saturates. Figure 6 shows the step response of the closed loop system for $r(t) = 10 * 1(t)$. Unstable limit cycle develops.

Second design step In the second design step we first build an equivalent linear system around the saturation block, using two new transfer functions C and H as shown in fig. 2 while imposing the equality $G = C/(1 + H)$. The linear transmission around the saturation block is $L_n = \{P\}C+H$. Then, by including the uncertainty of the saturation element, eq. (6), the design for limit-cycle avoidance is carried out by satisfying the condition

$$\{P\}C + H \neq -\frac{1}{\{N\}} \tag{7}$$

or equivalently

$$\{N\}(\{P\}C + H) \neq -1 \tag{8}$$

In practice, margins are added to the $-1/N(A)$ locus and to the -1 point, respectively, see section IV. The output of this design will be the C and H transfer functions. As mentioned above, the Circle or Popov criteria could possibly be used instead of $-1/N(A)$ for the design of $\{P\}C + H$.

If the second design step is successful, a closed loop system is achieved that satisfies the design specifications, [20], if the control signal does not saturate, and avoids limit cycling otherwise.

IV. Proposed solution

In this section an algorithm is given for the *second design step*.

Given G from the first design step. The design of C and H according to the Horowitz structure in fig. 2 proceeds as follows, such that

$$G = C\frac{1}{1+H} \tag{9}$$

and eq. (7), or equivalently eq. (8), hold with margins to be defined below. C is eliminated by combining eq. (9) and eq. (7) to yield

$$\{P\}G\,(1+H) + H \neq -\frac{1}{\{N\}} \tag{10}$$

where H is the unknown transfer function to be designed. Write eq. (10) as

$$\{N\}\left[\{P\}G\left(1+H\right)+H\right] \neq -1 \tag{11}$$

Rewriting eq. (11) as $1+\{N\}\left[\{P\}G\left(1+H\right)+H\right] \neq 0$ makes it clear that eq. (11) is equivalent to the "sensitivity" function specification

$$\left|\frac{1}{1+\{N\}\left[\{P\}G\left(1+H\right)+H\right]}\right| < \infty \tag{12}$$

In order to have some limit cycle avoidance margin, the right hand side in eq. (12) is replaced by a smaller gain, i.e.

$$\left|\frac{1}{1+\{N\}\left[\{P\}G\left(1+H\right)+H\right]}\right| \leq x\ dB \tag{13}$$

This equation is in standard QFT form for finding sensitivity bounds [21], [20]. Methods for multiplying and adding uncertain transfer functions in order to create composite templates can be found in e.g. [22], [23], [24].

Once H has been designed to satisfy eq. (13) for some x, C is computed from eq. (9) and the design is complete. In sections V and VI, detailed design examples are given.

V. Simulation example

The example is taken from [1]. Consider the control structure in fig. 2. An uncertain plant P is given with

$$P = 5\frac{(s/a+1)}{s(s/b+1)}\ ,\ a \in [0.5, 0.7]\ ,\ b \in [0.04, 0.1]. \tag{14}$$

The nominal parameter values are $a = 0.5$ and $b = 0.1$. The control input saturation in fig. 1 is $|u| \leq 1$. The nominal value for the uncertain gain of the describing function is taken as $N^*_{nom} = 1$. The compensators G and F are taken from [1]:

$$G = \frac{6s+5}{s}, \quad F = 1 \tag{15}$$

As in [1], the frequencies chosen for the computation of the templates and Horowitz-Sidi bounds are $\omega = [0.01, 0.1, 0.5, 1, 10]$ [rad/sec]. Our solution yields

$$H = \frac{-1}{s/3+1}. \tag{16}$$

from which eq. (9) gives

$$C = \frac{6s+5}{s+3}, \quad . \tag{17}$$

Figure 7 shows some computed bounds for the design of H to satisfy eq. (13) for x=10, for the frequencies $0.5, 1, 10$ [rad/sec] together with the designed H transfer function. Clearly, all the displayed bounds are satisfied. Figure 8 verifies that eq. (7) is satisfied for some plant cases.

Comparing our step responses in fig. 10, with the corresponding step responses from [1] in fig. 9 reveals that the response time of the proposed solution is seemingly decreased by approximately five times, at a price of an overshoot.

It should be noted that our step responses are identical to those in fig. 24 in [1] generated by the classical ARW

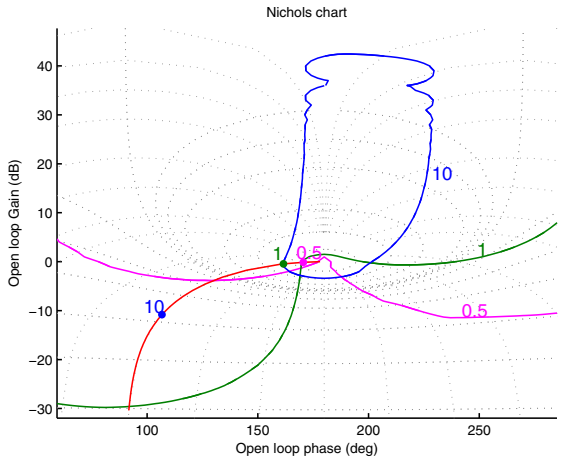

Fig. 7. Design of H (red graph) with Horowitz-Sidi bounds in a Nichols chart for $\omega = 0.5, 1, 10$ [rad/sec]. The Horowitz-Sidi bounds are satisfied if the frequency function values at the given frequencies do not reside in their respective forbidden sets to which the instability point -1(0 dB, -180 deg) belongs.

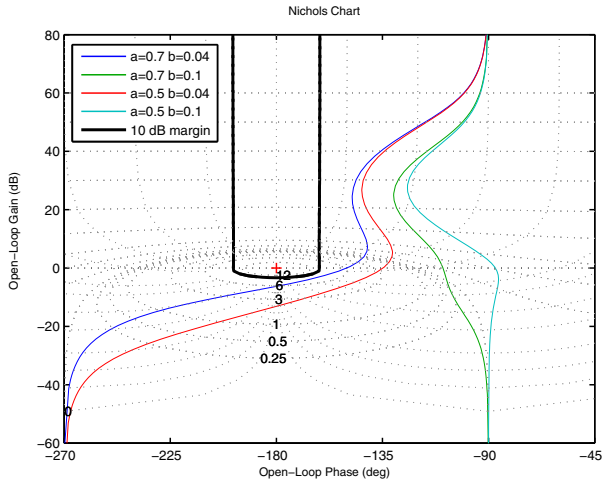

Fig. 8. Nichols plot of $PC + H$ for various plant cases, and $-1/\{N\}$ with 10 [dB] margin. Grid shown is for the sensitivity transfer function, eq. (13).

structure in fig. 8 in [1]. This does not come as a surprise since our design is identical to the PI design in fig. 8 of [1] with $T_r = 1/3$, $K_p = 6$ and $T_I = 1.2$. The more common choice of $T_r = T_I = 1.2$ would yield $H = -1/(1+1.2s)$ and $C = K_p = 6$ which also satisfies the Describing Function limit cycle avoidance condition.

VI. Real design example

An X-Y stage used for the wafer metrology industry is considered, fig. 11. Plant frequency response data in the Y-direction were collected at various sinusoidal excitation amplitudes, with current reference [A] to the existing current loop as input and linear encoder position [mm] as output. The system is characterized by large uncertainty in the low frequency range, caused mainly by friction [25], [26], [27].

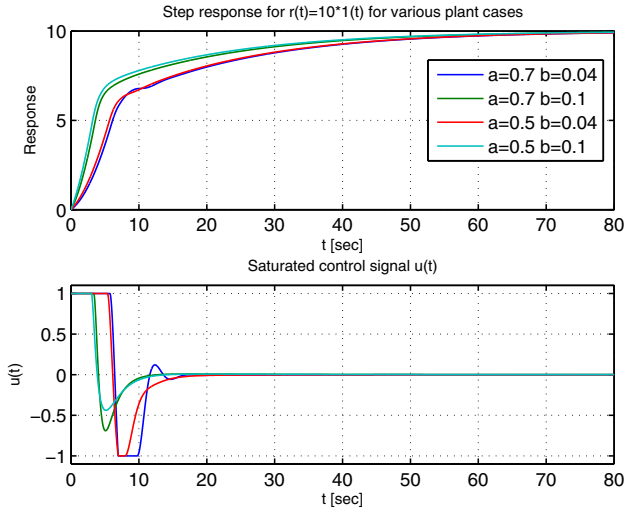

Fig. 9. Taken from [1]. Simulated closed loop step responses for $r(t) = 10 * 1(t)$, and the saturated control signal $u(t)$, for various plant cases eq. (14). The structure is found in fig. 3, with G and F given by eq. (15), and $E = (100.25s + 20)/(s(s + 0.05))$.

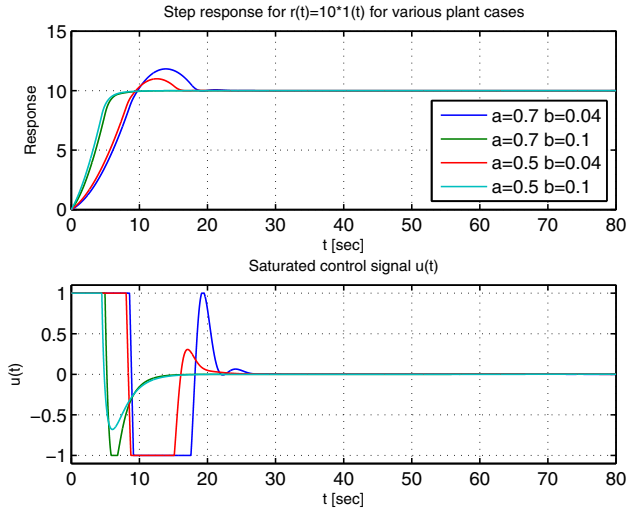

Fig. 10. Simulated closed loop step response using the proposed solution in fig. 2, C and H given by eqs. (16) and (17), for $r(t) = 10 * 1(t)$ and the saturated control signal $u(t)$ for various plant cases, eq. (14).

Five measured plant cases are shown in fig. 12. In the first design step, the system is configured as in fig. 1 and G and F are designed. Given the sensitivity specification $|1/(1 + \{P\}G)| < 6$ [dB], a minimum cross-over frequency specification, $\omega_{cmin} = 1000$ [rad/s], and the first stiffness coefficient $c_0 = 0$, a specification satisfying feedback compensator G was designed

$$G = \frac{10^4(s/500 + 1)(s^2/217^2 + 2 \cdot 0.68 \cdot s/217 + 1)}{s(s^2/1000^2 + 2 \cdot 0.9 \cdot s/1000 + 1)} \tag{18}$$

The prefilter was chosen as $F = 1$. With the nominal plant case P_{nom} as indicated in fig. 12, the nominal open loop $L_{nom} = P_{nom}G$ is shown in fig. 13, where it is noted that the

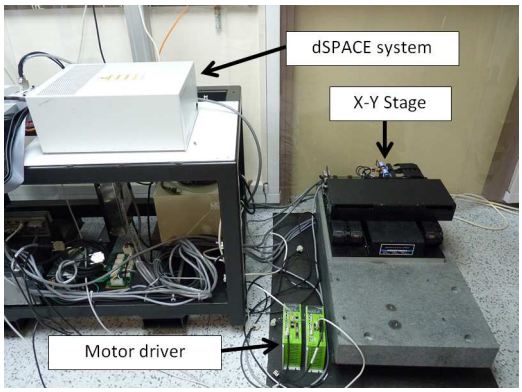

Fig. 11. Setup for X-Y Stage together with the dSPACE system and the motors drivers.

nominal closed loop system is conditionally stable. Figure 14 shows the measured step response for $r(t) = 5 * 1(t)$. The response exhibits unstable limit cycles.

In the second design stage the structure in fig. 2 is used. Horowitz-Sidi bounds for the design of H were computed, and H was designed to satisfy eq. (13) with $x = 12$, resulting in

$$H = \frac{-1}{s/1250 + 1}. \tag{19}$$

Figure 15 verifies the satisfaction of bounds for two frequencies. C is then computed from eqs. (9) and (19) to yield

$$C = \frac{10^4(s/500 + 1)(s^2/217^2 + 2 \cdot 0.68 \cdot s/217 + 1)}{(s + 1250)(s^2/1000^2 + 2 \cdot 0.9 \cdot s/1000 + 1)} \tag{20}$$

Figure 16 shows that eq. (7) is satisfied for the five plant cases. Figures 17 and 18 show that the sufficient Popov and Circle criteria are not satisfied, thus global stability is not assured by these criteria.

Finally, fig. 19 shows the measured step response to $r(t) = 5 * 1(t)$, with the modified control structure, fig. 2. No limit cycles are present.

VII. Design and Implementation Issues

For controlling the stage, a dSPACE environment is used for the digital controller implementation and measurements. A linear encoder manufactured by Renishaw is used as the feedback position sensor with a resolution of 5 [nm]. The sampling frequency is set to 10 [kHz]. An analog voltage command is the output of the dSPACE system, used as current reference for the motor driver current loop. A digital motor driver, manufactured by Mega-Fabs Motion Systems Ltd. is used to control the three phase linear motor.

In the following, some remarks regarding the design and implementation are given.

1) Consider the case when there are two or three integrators in $\{P\}G$. Then $\{P\}G$ will always intersect $-1/\{N\}$, see figs. 5 and 13. Now consider eq. (10) rewritten as

$$(\{P\}G + 1)H + \{P\}G \neq -1/N. \tag{21}$$

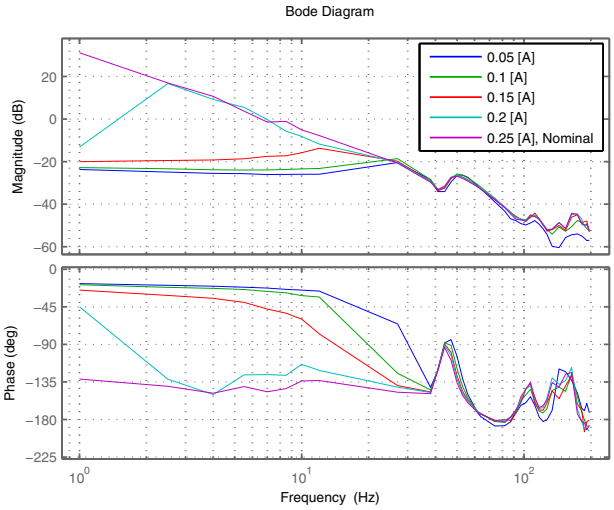

Fig. 12. Measured Bode plots for five X-Y stage plant cases for different excitation amplitudes. The chosen nominal plant is indicated.

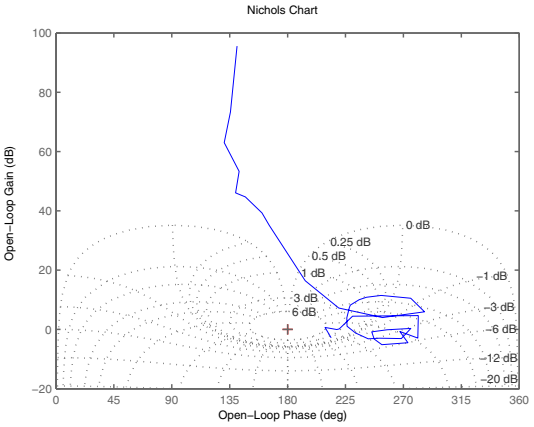

Fig. 13. Nichols plot for L_{nom}, eq. (3), of the first design step, fig. 1. The nominal plant is shown in fig. 12, G is given in eq. (18) and $F = 1$.

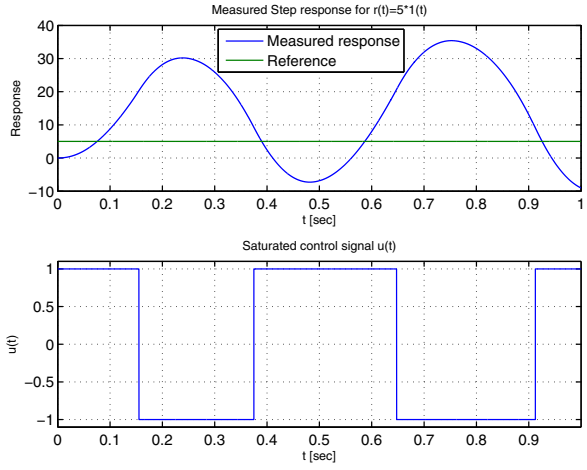

Fig. 14. Measured closed loop step response for $r(t) = 5 * 1(t)$ and the saturated control signal $u(t)$. The configuration is given in fig. 1, with G from eq. (18) and $F = 1$. An unstable limit cycle develops.

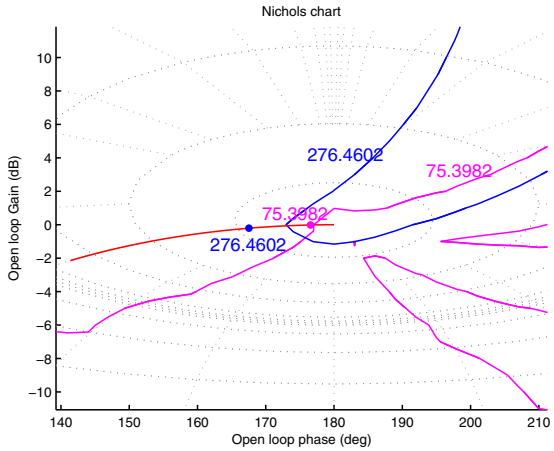

Fig. 15. Design of H (red graph) with Horowitz-Sidi bounds in a Nichols chart for $\omega = 75.3, 276.4$ [rad/sec]. The Horowitz-Sidi bounds are satisfied since the nominal frequency function values at the given frequencies do not reside in their respective forbidden sets to which the instability point -1(0 dB, -180 deg) belongs.

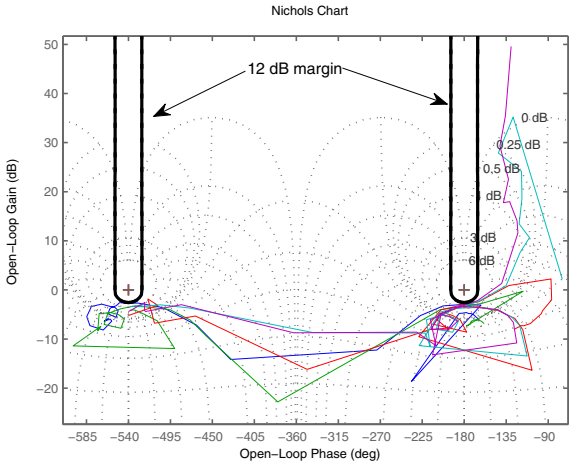

Fig. 16. Nichols plot for five $PC + H$ cases, and $-1/\{N\}$ with $12dB$ margin.

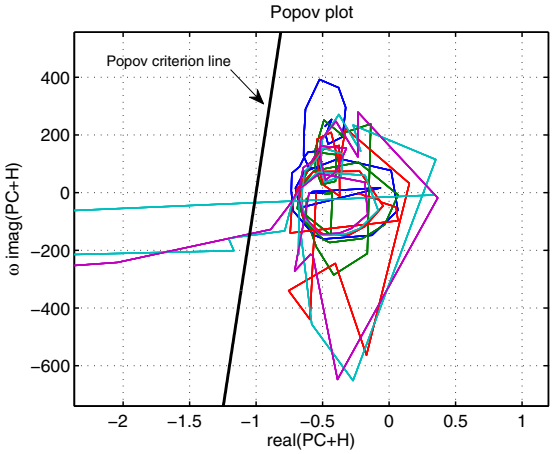

Fig. 17. Popov plot for five transformed $PC + H$ cases with Popov criterion line.

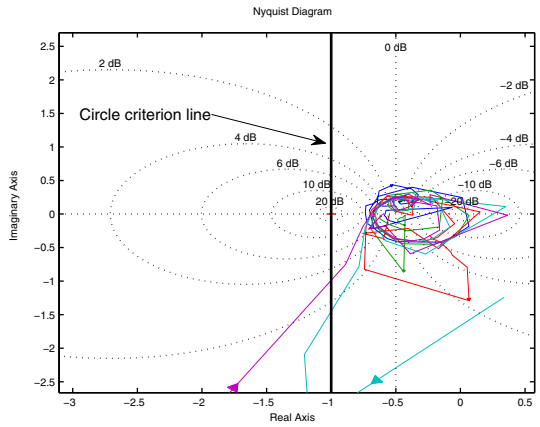

Fig. 18. Nyquist plot for five $PC + H$ cases with Circle criterion line

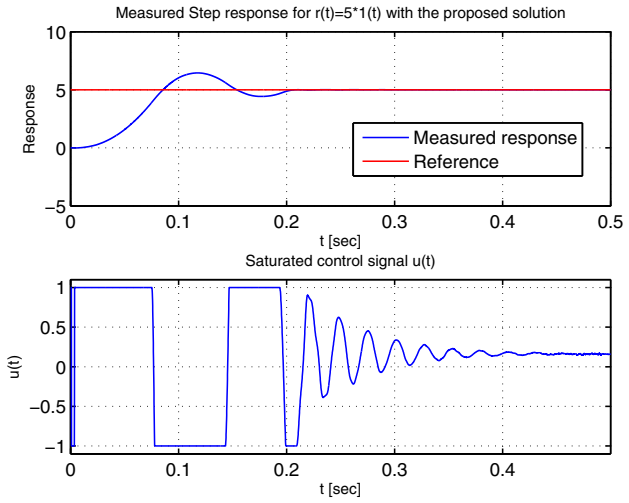

Fig. 19. Measured step response for $r(t) = 5 * 1(t)$ with the proposed solution, fig. 2, together with the saturated control signal $u(t)$. C and H are given by eqs. (19) and (20). Limit cycle does not develop.

where the choice of $H(s)$ such that $H(0) = -k$, $k \geq 1$ makes it possible to avoid the intersection between the left hand side of eq. (21) and the straight line [$\pm\infty$ db, -180 deg] in the Nichols chart for $s = j\omega$, $\omega \geq 0$.

2) When designing H, one must take care that there is no unstable pole-zero cancellation in $G = C/(1+H)$. E.g. consider $H = -k/(1 + s/3))$ with $k \geq 1$ according to point 1 above. Then $1/(1 + H) = (1 + s/3)/(1 - k + s/3)$. There is no unstable pole-zero cancellation with $k \leq 1$. Hence $k = 1$ is the only choice. As a result $1/(1 + H)$ implements an integrator in G. If no integrator in G is desired, it may be canceled by a factor s in the numerator of C.
3) In order to avoid an algebraic loop in the feedback path of H, it is required that H be strictly proper. The bilinear (Tustin) transformation from analog to digital form should not be used, since it leads to a proper realization. Using the "Pole-zero matched" transformation [28] together with ZOH phase correction [29] is recommended.
4) An eventual feedforward signal could enter the loop at a summation point before the saturation, appropriately filtered. One possible structure is shown in fig. 20.

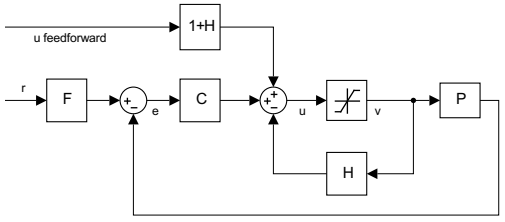

Fig. 20. Proposed structure for feedforward implementation

VIII. Conclusions

This paper addresses the problem of limit cycles avoidance in uncertain LTI systems with actuator input saturation. A two step quantitative feedback design procedure for uncertain systems using the QFT theory and the Describing Function method is shown in detail, whereby it is pointed out that the Popov and Circle criteria could possibly also be used. Two examples are given. In one example the equivalence between the presented method and classical ARW is demonstrated. A real-life example of the high performance control of a stage positioning system demonstrates the efficiency of the proposed method.

References

[1] J. C. Moreno, A. Banos, and M. Berenguel, "A qft framework for antiwindup control systems design," *Journal of Dynamic Systems, Measurement, and Control*, vol. 132, no. 2, pp. 021 012–021 012, Feb. 2010. [Online]. Available: http://dx.doi.org/10.1115/1.4000812

[2] H. A. Fertik and C. W. Ross, "Direct digital control algorithm with anti-windup feature," *ISA transactions*, vol. 6, no. 4, pp. 317–328, 1967.

[3] J. C. Doyle, R. S. Smith, and D. Enns, "Control of plants with input saturation nonlinearities," in *American Control Conference, 1987*, 1987, pp. 1034–1039.

[4] R. Hanus, M. Kinnaert, and J.-L. Henrotte, "Conditioning technique, a general anti-windup and bumpless transfer method," *Automatica*, vol. 23, no. 6, pp. 729–739, Nov. 1987. [Online]. Available: http://www.sciencedirect.com/science/article/pii/000510988790029X

[5] M. V. Kothare, P. J. Campo, M. Morari, and C. N. Nett, "A unified framework for the study of anti-windup designs," *Automatica*, vol. 30, no. 12, pp. 1869–1883, Dec. 1994. [Online]. Available: http://www.sciencedirect.com/science/article/pii/0005109894900485

[6] I. Horowitz, "Quantitative feedback theory," *Control Theory and Applications, IEE Proceedings D*, vol. 129, no. 6, pp. 215–226, 1982, iD: 1.

[7] ——, "A synthesis theory for a class of saturating systems," *International Journal of Control*, vol. 38, no. 1, pp. 169–187, July 1983. [Online]. Available: http://www.tandfonline.com/doi/abs/10.1080/00207178308933067

[8] J. C. Moreno, A. Banos, and M. Berenguel, "A synthesis theory for uncertain linear systems with saturation," in *Proceedings of the Fourth IFAC Symposium on Robust Control Design, Milan, Italy*, 2003.

[9] M. A. Franchek and P. A. Herman, "Direct connection between time-domain performance and frequency-domain characteristics," *Int. J. Robust Nonlinear Control*, vol. 8, no. 12, pp. 1021–1042, 1998. [Online]. Available: http://dx.doi.org/10.1002/(SICI)1099-1239(1998100)8:12<1021::AID-RNC363>3.0.CO;2-S

[10] S. Oldak, C. Baril, and P. O. Gutman, "Quantitative design of a class of nonlinear systems with parameter uncertainty," *Int. J. Robust Nonlinear Control*, vol. 4, no. 1, pp. 101–117, 1994. [Online]. Available: http://dx.doi.org/10.1002/rnc.4590040108

[11] G. Zames and P. Falb, "Stability conditions for systems with monotone and slope-restricted nonlinearities," *SIAM Journal on Control*, vol. 6, no. 1, pp. 89–108, 1968.

[12] W. Wu and S. Jayasuriya, "A new qft design methodology for feedback systems under input saturation," *Journal of Dynamic Systems, Measurement, and Control*, vol. 123, no. 2, pp. 225–232, Oct. 2001. [Online]. Available: http://dx.doi.org/10.1115/1.1367337

[13] J. Moreno, G. J.L., A. Banos, and M. Berenguel, "The input amplitude saturation problem in qft: A survey," *Annual Reviews in Control*, vol. 35, no. 1, pp. 34–55, Apr. 2011. [Online]. Available: http://www.sciencedirect.com/science/article/pii/S1367578811000034

[14] E. Villota, M. Kerr, and S. Jayasuriya, "A study of configurations for anti-windup control of uncertain systems," in *Decision and Control, 2006 45th IEEE Conference on*, 2006, pp. 6193–6198.

[15] A. Gelb and W. E. V. Velde, *Multiple-Input Describing Functions and Nonlinear System Design*. McGraw Hill, 1968.

[16] A. Lichtsinder, "Reciprocity of friction and backlash in servo control systems," Ph.D. dissertation, Technion - Israel Institute of Technology, 2014.

[17] A. Banos and A. Barreiro, "Stability of non-linear qft designs based on robust absolute stability criteria," *International Journal of Control*, vol. 73, no. 1, pp. 74–88, Jan. 2000. [Online]. Available: http://dx.doi.org/10.1080/002071700219957

[18] A. Banos, A. Barreiro, F. Gordillo, and J. Aracil, "A qft framework for nonlinear robust stability," *Int. J. Robust Nonlinear Control*, vol. 12, no. 4, pp. 357–372, 2002. [Online]. Available: http://dx.doi.org/10.1002/rnc.653

[19] E. Eitelberg and E. Boje, "Some practical low frequency bounds in quantitative feedback design," in *Control and Applications, 1989. Proceedings. ICCON '89. IEEE International Conference on*, 1989, pp. 511–515.

[20] I. Horowitz, *Quantitative Feedback Design Theory: (QFT)*. QFT Pub., 1993. [Online]. Available: http://books.google.co.il/books?id=3ZRSAAAAMAAJ

[21] P. Gutman, "Qsyn, the toolbox for robust control systems design for use with matlab," *User's manual, www.math.kth.se/optsyst/forskning/forskarutbildning/5B5782/*, 1996.

[22] A. Rantzer and P. O. Gutman, "Algorithm for addition and multiplication of value sets of uncertain transfer functions," in *Decision and Control, 1991., Proceedings of the 30th IEEE Conference on*, 1991, pp. 3056–3057 vol.3.

[23] P. O. Gutman, C. Baril, and L. Neumann, "An algorithm for computing value sets of uncertain transfer functions in factored real form," *Automatic Control, IEEE Transactions on*, vol. 39, no. 6, pp. 1268–1273, 1994.

[24] P.-O. Gutman, M. Nordin, and B. Cohen, "Recursive grid methods to compute value sets and horowitzsidi bounds," *Int. J. Robust Nonlinear Control*, vol. 17, no. 2-3, pp. 155–171, 2007. [Online]. Available: http://dx.doi.org/10.1002/rnc.1083

[25] C. G. Baril and P. O. Gutman, "Performance enhancing adaptive friction compensation for uncertain systems," *Control Systems Technology, IEEE Transactions on*, vol. 5, no. 5, pp. 466–479, 1997, iD: 1.

[26] F. Al-Bender and J. Swevers, "Characterization of friction force dynamics," *Control Systems, IEEE*, vol. 28, no. 6, pp. 64–81, 2008, iD: 1.

[27] B. Armstrong-Helouvry and P. Dupont, "Friction modeling for control," in *American Control Conference, 1993*, 1993, pp. 1905–1909, iD: 1.

[28] N. Hori, J. Cormier, R., and K. Kanai, "Matched pole-zero discrete-time models," *Control Theory and Applications, IEE Proceedings D*, vol. 139, no. 3, pp. 273–278, 1992.

[29] D. Raviv and E. Djaja, "Technique for enhancing the performance of discretized controllers," *Control Systems, IEEE*, vol. 19, no. 3, pp. 52–57, 1999.